

Working Title: Monte Carlo Analysis of Dynamic Systems

by

Chelsea A. D'Angelo

A preliminary report submitted in partial fulfillment of
the requirements for the degree of

Doctor of Philosophy

(Nuclear Engineering and Engineering Physics)

at the

UNIVERSITY OF WISCONSIN-MADISON

2017

Date of preliminary oral examination: 09/01/2017

Thesis Committee:

Paul P. H. Wilson, Professor, Nuclear Engineering

Douglass Henderson, Professor, Nuclear Engineering

Bryan Bednarz, Professor, Medical Physics

Andrew Davis, Associate Scientist, Engineering Physics

© Copyright by Chelsea A. D'Angelo 2017
All Rights Reserved

CONTENTS

Contents	i
List of Figures	iii
1 Introduction	2
2 Literature Review	5
2.1 <i>Analog Monte Carlo Calculations</i>	6
2.2 <i>Shutdown Dose Rate Analysis</i>	7
2.2.1 D1S	7
2.2.2 R2S	8
2.2.2.1 Mesh-based R2S	8
2.3 <i>Monte Carlo Variance Reduction Methods</i>	9
2.4 <i>Automated Variance Reduction</i>	11
2.4.1 CADIS	13
2.4.2 FW-CADIS	14
2.5 <i>Automated Variance Reduction for Multi-physics Analysis</i> . . .	15
2.5.1 MS-CADIS	16
2.5.2 GT-CADIS	18
2.6 <i>Moving Geometries and Sources</i>	19
2.6.1 MCNP6 Moving Objects Capability	19
2.6.2 MCR2S with Geometry Movement	20
3 Experiment	21
3.1 <i>Demonstration of GT-CADIS</i>	21
3.1.1 Problem Description	21
3.1.2 Analog R2S	22
3.1.3 GT-CADIS	23
3.2 <i>Limitations of GT-CADIS for Moving Systems</i>	27

4	Variance Reduction for Time-integrated Multiphysics Analysis	34
4.1	<i>Generalized MS-CADIS Method</i>	34
4.2	<i>Time-integrated MS-CADIS</i>	37
4.3	<i>Time-integrated GT-CADIS</i>	38
5	Proposal	40
5.1	<i>Progress: DAGMC Simulations with Geometry Transformations</i>	40
5.1.1	Production of Stepwise Geometry Files	41
5.1.2	DAGMCNP Geometry Transformations	41
5.2	<i>Implementation Plan: Time-integrated SDR Analysis</i>	42
5.2.1	Time-integrated R2S	42
5.2.2	Generation of the TGT-CADIS Variance Reduction Parameters	43
5.2.3	Fully-optimized, Time-integrated R2S Workflow . .	47
5.2.4	Error Propagation	48
5.2.5	Assumptions and Practical Considerations	50
5.2.5.1	Data management	51
5.3	<i>Demonstration</i>	52
5.3.1	Toy Problem	52
5.3.2	Full-scale FES Model	53
5.4	<i>Summary</i>	53
	Bibliography	54

LIST OF FIGURES

3.1	Experimental Geometry	22
3.2	Analog neutron flux and error	24
3.3	Analog photon source	25
3.4	GT-CADIS adjoint photon flux	26
3.5	GT-CADIS adjoint neutron flux	27
3.6	GT-CADIS biased neutron source	28
3.7	GT-CADIS weight window mesh	29
3.8	GT-CADIS neutron flux and relative error	30
3.9	GT-CADIS photon source	31
3.10	Path of moving component	32
3.11	Adjoint neutron flux map with region of moving component highlighted.	33
5.1	Time-integrated R2S (TR2S) workflow	44
5.2	Workflow to generate TGT-CADIS adjoint neutron source . . .	46
5.3	Workflow to generate TGT-CADIS biased source and weight windows	47
5.4	Fully optimized, time-integrated R2S workflow	49
5.5	Geometry for TGT-CADIS Demonstration	52

Abstract

Abstract

Eloquent summary of my work.

TODO LIST

do I mention deterministic anywhere else?	6
Should I explain why this is prop. to $1/\sqrt{N}$?	6
Add subsection to introduce mesh-based R2S and PyNE R2S [9] . .	8
Wording: want to clearly make distinction btwn PDFs of actual, physical particle behavior and biased PDFs that modify real behavior	10
Need to discuss pro/con of deterministic/MC in earlier section . .	11
Need to label this figure	22
Show these figures on the same page so they are easily compared. Probably regenerate them so they have the same limits on the color bar	27
Label orig location, final location, detector. Make central cavity white to indicate there is no longer a neutron source here	28
Are these two statements strong enough? This is the whole point of the work.	29
Arrange figures so they appear closer to text describing them. . . .	29
Not sure if this is clear.	35
Change to time-dependent? Time-integrated gives the impression that the SDR at each time step will be averaged together to give a total dose during the movement. What is more useful? Separate SDR map at each time step or a single, averaged dose? .	42
This might need to be explained better. Maybe a picture showing showing mapping of voxel to tet mesh	45
should I use separate subscript for voxel?	45
Is $q_{\gamma, t_{dec}, t_{mov}}$ defined properly in text?	48
This is shown in Elliott's prelim, but not thesis. Is this still an appro- priate way to calculate the FOM?	50
Missing demo figure	52

1 INTRODUCTION

The successful completion of this project will provide the workflow and tools necessary to efficiently calculate quantities of interest resulting from coupled, multi-physics processes in dynamic systems. The driving force behind this work is the quantification of the shutdown dose rate (SDR) resulting from the coupled neutron irradiation-photon emission that occurs in fusion energy systems (FES); specifically investigating how to optimize the SDR calculation when activated system components are moved during maintenance activities. The Monte Carlo radiation transport code will be modified to implement rigid-body transformations on the CAD-based geometry. MS-CADIS, a VR method for coupled, multi-physics problems, will be adapted to incorporate dynamics. An experiment will be contrived to demonstrate the limitations of existing VR methods as they apply to dynamic problems and verify the efficacy of this new method. Given these objectives, the Chapter 2 will include background and theory relevant to VR methods in coupled, multi-physics systems. It begins with an introduction to computational radiation transport, specifically the Monte Carlo method. It will then introduce the methods currently used for SDR analysis and the need for optimization. Several MC VR techniques and how they have been applied to optimize SDR analysis are then discussed. Finally, this chapter ends with a discussion about radiation transport in dynamic systems. Next, Chapter 3 shows the experiment demonstrating the need for a new VR method to optimize the SDR in dynamic systems. The derivation of VR parameters that will optimize the SDR in dynamic systems is given in Chapter 4 and an implementation plan in Chapter 5. Chapter 5 will also discuss the progress that has been made towards this new methodology and summarize the work to be done.

The rapid design iteration process of complex nuclear systems has long been aided by the use of computational simulation. Traditionally, these

simulations involve radiation transport in static geometries. However, in certain scenarios, it is desirable to investigate dynamic systems and the effects caused by the motion of one or more components. For example, FES are purposefully designed with modular components that can be moved in and out of a facility after shutdown for maintenance. To ensure the safety of maintenance personnel, it is important to accurately quantify the SDR caused by the photons emitted by structural materials that were activated during the device operation time. This type of analysis requires neutron transport to determine the neutron flux, activation analysis to determine the isotopic inventory, and finally a photon transport calculation to determine the SDR. While MC calculations are revered to be the most accurate method for simulating radiation transport, the computational expense of obtaining results with low error in systems with heavy shielding can be prohibitive. However, VR methods can be used to increase the computational efficiency. There are several types of VR methods, but the basic theory is to artificially increase the simulation of events that will contribute to the quantity of interest such as flux or dose rate. One class of VR techniques relies upon a deterministic estimate of the adjoint solution of the transport equation to formulate biasing parameters to accelerate the MC transport. The adjoint flux has physical significance as the importance of a region of phase space to the objective function.

For cases involving coupled multi-physics analysis in dynamics systems, such as SDR calculations during maintenance activities, a new hybrid deterministic/MC VR technique will be proposed. This new method will adapt the Multi-Step Consistent Adjoint Driven Importance Sampling (MS-CADIS) method to dynamic systems. The basis of MS-CADIS is that the importance function used in each step of the problem must represent the importance of the particles to the final objective function. As the spatial configuration of the materials changes, the probability that they will contribute to the objective function also changes. In the specific case of SDR

calculations, the importance function for the neutron transport step must capture the probability of materials to become activated and subsequently emit photons that will make a significant contribution to the SDR. This new VR method will also adapt the Groupwise Transmutation (GT)-CADIS method which is an implementation of MS-CADIS that optimizes the neutron transport step of SDR calculations. GT-CADIS generates an adjoint neutron source based on certain assumptions and approximations about the transmutation network. To adapt this method for dynamic systems, a time-integrated adjoint neutron source will be calculated in order to generate the biasing functions for the neutron transport step.

2 LITERATURE REVIEW

The goal of this thesis work is to optimize the initial radiation transport step of a coupled, multi-physics process occurring in a system that has moving components. One important application of this work is the quantification of the shutdown dose rate (SDR) during maintenance operations in fusion energy systems (FES).

During the operation of a fusion device, the nuclear reactions (e.g. D-T fusion) occurring in the plasma result in the production of high energy (14 MeV) neutrons that penetrate deeply into the system components. Some of the neutron reaction pathways result in the production of radioisotopes that persist long after device shutdown. The activated components emit high energy photons as they reach stability over time. These high energy photons can cause grave health effects, therefore it is necessary to quantify the dose rate in order to ensure the safety of personnel working in fusion facilities. This is not only important for the time during operation and immediately after shutdown when the device is in a static configuration, but also during a maintenance activity when activated components are moving around the facility and the dose rate is changing over time.

Performing computational simulations of the radiation transport in these devices and calculating quantities of interest, such as flux and dose rate, are a crucial part of the fusion reactor design phase. These simulations can inform decisions about the sustainability and safety of the device. This chapter will provide background on computational radiation transport, methods for SDR analysis, methods for optimizing radiation transport calculations, and finally how radiation transport calculations are currently handled in systems with moving geometries and sources.

2.1 Analog Monte Carlo Calculations

The quantification of the SDR requires a detailed distribution of the neutron and photon flux throughout all regions of phase space (space, energy, and direction). Due to the size and complexity of FES, the most optimal way to obtain accurate particle distributions is through Monte Carlo (MC) radiation transport rather than deterministic methods.

In general, MC calculations rely on repeated random sampling to solve mathematical problems. In radiation transport applications, the MC method is used to solve the Boltzmann transport equation [15] through the simulation of random particle walks through phase space. In analog operation mode (i.e. no variance reduction), the source particle's position, energy, direction, and subsequent collisions are sampled from unbiased probability distribution functions (PDFs) that describe physical particle behavior. The particle's journey through space, or history, is tracked until it is terminated. Quantities of interest such as flux can be scored, or tallied, by averaging particle tracks in discrete regions of phase space.

do I mention deterministic anywhere else?

One challenge incurred by MC simulations of FES is the presence of heavily shielded regions. The particles undergo a high degree of collisions (absorption and scattering) in the shielding which results in low particle fluxes in the attenuated regions. Regions that have low particle fluxes are sampled less frequently and therefore have higher statistical uncertainty than regions with high flux that are sampled very often.

This uncertainty can be represented by the relative error, \mathfrak{R} , which is defined as the statistical precision, \bar{x} (the average of the tally scores), divided by the mean, $\sigma_{\bar{x}}$ (the standard deviation of the tally scores).

$$\mathfrak{R} = \frac{\sigma_{\bar{x}}}{\bar{x}} \quad (2.1)$$

For a well behaved, properly converged tally, \mathfrak{R} is proportional to $1/\sqrt{N}$ where N is the number of histories [3]. Therefore, to reduce the uncertainty,

Should I explain why this is prop. to $1/\sqrt{N}$?

one can increase the number of particle histories simulated. Compute time scales linearly with N , and \mathfrak{R} is inversely proportional to \sqrt{N} , therefore to reduce the error by half, the number of histories, and therefore time, required will quadruple.

The efficiency of MC calculations is measured by a quantity known as the figure of merit (FOM). The FOM is a function of relative error, \mathfrak{R} , and computer processing time, t_{proc} , as given by

$$\text{FOM} = \frac{1}{\mathfrak{R}^2 t_{\text{proc}}} \quad (2.2)$$

A high FOM is desirable because it means that less computation time is needed to achieve a reasonably low error (>0.1 [3]).

2.2 Shutdown Dose Rate Analysis

This section will discuss the two primary workflows used to investigate the SDR: the Direct 1-Step (D1S) [4] and the Rigorous 2-Step (R2S) [7] method. Both methods couple the neutron and photon transport via activation analysis to calculate the SDR.

2.2.1 D1S

As its name implies, the D1S method performs coupled neutron-photon transport in a single simulation. It relies upon a version of the MC code, MCNP5 [3], that has slight modifications as well as special cross-section data that replaces prompt gammas with decay gammas. When a prompt photon reaction is sampled in a standard MCNP simulation, the photon is stored until the original neutron transport is completed. Then, the photon is transported as part of the same simulation. The version of MCNP5 used by D1S allows the delayed photons to be emitted as prompt so they can be transported in the same simulations as neutrons. A time correction

factor calculated with FISPACT [5] is later applied. The Advanced D1S [6] includes improvements to allow for the calculation of dose rate on a 3D mesh. Because both neutron and photon transport occur in the same simulation, therefore on the same geometry, D1S is not currently applicable to geometries that undergo movement after shutdown. This has been identified as a necessary improvement and the development of a subroutine to produce portable decay photon sources for pure photon calculations is underway [6].

2.2.2 R2S

In contrast to D1S, the R2S method relies upon separate MC neutron and photon transport simulations. The transport steps are coupled through activation analysis by a nuclear inventory code. The goal of the neutron transport step is to determine the neutron flux as a function of space and energy. This neutron flux along with a specific irradiation and decay scenario are used as input into a nuclear inventory code to determine the photon emission density as a function of decay time. The calculated photon emission density for each decay time is then used as the source for MC photon transport. A photon flux tally fitted with flux-to-dose-rate conversion factors is used to determine the final SDR [7]. Because the neutron and photon transport are performed in separately, different geometries can be used for each transport step which is key for simulating geometry movement after shutdown.

2.2.2.1 Mesh-based R2S

In order to calculate an accurate dose rate, it is necessary to obtain detailed distributions of the neutron flux and photon source throughout the geometry. The Mesh-tally Coupled R2S (MCR2S) tool was the first implementation of a mesh-based R2S methodology [8]. It couples MCNP

Add subsection to introduce mesh-based R2S and PyNE R2S [9]

neutron and photon transport calculations with the FISPACT nuclear inventory code. First, multi-group neutron fluxes are scored on a 3D mesh. Then, the geometry used for MC transport is discretized onto a mesh, a requirement of activation codes. Using the mesh-based geometry/material description, multi-group neutron fluxes, and irradiation and decay scenario, the inventory code calculates the photon emission density in each mesh element for each decay time [8]. These photon emission density distributions are then used as sources for MC photon transport simulations.

The Python for Nuclear Engineering (PyNE) toolkit has many useful functions and scripts to assist in nuclear analysis [23]. PyNE has an R2S module [9] that includes functions and scripts to implement the mesh-based R2S method for CAD geometries. It relies on the Direct Accelerated Geometry Monte Carlo (DAGMC) toolkit and an MC code, such as MCNP, for neutron and photon transport and ALARA [20] for nuclear inventory analysis. The DAGMC toolkit allows MC transport to be performed directly on CAD geometry.

2.3 Monte Carlo Variance Reduction Methods

As mentioned in section 2.1, the presence of highly attenuating structural materials in FES presents a challenge for MC calculations. Regions with low particle fluxes are not sampled as frequently and therefore have higher statistical uncertainty associated with results scored there. A set of techniques, known as variance reduction (VR), can be used to decrease the statistical uncertainty in these results in a more efficient way than the brute force method of increasing the number of particle histories. VR methods aim to increase the FOM, a measure of efficiency given in Eq. 2.2, by reducing the compute time necessary to achieve a statistically reasonable result. This is done by modifying particle behavior to preferentially

sample trajectories that are likely to contribute to the tallies of interest.

One way this is accomplished is by sampling from biased PDFs instead of the standard PDFs used in analog calculations that describe actual particle behavior. In order to compensate for this biased sampling, the particle statistical weight is adjusted as follows [1]

$$w_{\text{biased}} \text{pdf}_{\text{biased}} = w_{\text{unbiased}} \text{pdf}_{\text{unbiased}} \quad (2.3)$$

If the biased sampling results in an event occurring more frequently than it does in reality, the particle weight is decreased and vice versa. Sampling from biased PDFs to preferentially sample events that will result in an increased number of histories that contribute to the tally of interest can decrease the standard deviation, and therefore relative error, \mathfrak{R} , which will increase the FOM.

Another method of VR is particle splitting and rouletting. To increase the number of particle histories that can contribute to a tally of interest, it is desirable to split particles as they enter more important regions and roulette particles as they enter less important regions. The decision to split or roulette particles first requires assigning an importance, I , to every region in the geometry. When a particle moves from a region A to a region B, the ratio of importances is calculated. If region B is more important than region A such that $I_B/I_A \geq 1$, the particle with original weight w_0 is split into $n = I_B/I_A$ particles, each with weight w_0/n . If instead region B is less important than region A such that $I_B/I_A < 1$, the particle will undergo roulette. The particle will survive with a probability n and weight w_0/n [2]. This is particularly useful in calculating results in heavily attenuated regions, like in FES. Importances can be assigned in a way that will force particle flow towards the region of interest.

The weight window method in the Monte Carlo N-Particle (MCNP) code utilizes both splitting and rouletting. A weight window is a region of phase-space that is assigned an upper and lower bound. The windows

Wording:

want to clearly make distinction btwn PDFs of actual, physical particle behavior and biased PDFs that modify real behavior

can be assigned to cells in the geometry, on a superimposed mesh, and to energy bins. When a particle enters a weight window, its weight is assessed; if its weight is above the upper bound, it is split and if it is below the lower bound, it is rouletted. There are various methods to produce these weight window bounds automatically which drastically reduces the time, effort, and expertise required by the analyst. Some of these methods will be discussed in the following section.

2.4 Automated Variance Reduction

Historically, VR techniques have required a priori knowledge of the problem physics in order to assign modified sampling and weight control parameters. Many techniques have been developed over the years to automate the selection and assignment of these parameters to reduce computational and human effort.

One class of VR techniques, known as hybrid deterministic/MC methods, takes advantage of the speed of deterministic transport to estimate a solution to the adjoint Boltzmann transport equation which can then be used to generate MC VR parameters. The adjoint solution has significance as the measure of importance of a particle to some specified objective function. To demonstrate the use of the adjoint solution as an importance function, first start with the operator form of the linear, time-independent Boltzmann transport equation [15]

$$H\Psi(\vec{r}, E, \hat{\Omega}) = q(\vec{r}, E, \hat{\Omega}) \quad (2.4)$$

where Ψ is the angular flux, q is the source of particles, and the operator H which describes all particle behavior is given by

$$H = \hat{\Omega} \cdot \nabla + \sigma_t(\vec{r}, E) - \int_0^\infty dE' \int_{4\pi} d\Omega' \sigma_s(\vec{r}, E' \rightarrow E, \hat{\Omega}' \rightarrow \hat{\Omega}) \quad (2.5)$$

Need to discuss pro/con of deterministic/MC in earlier section

where σ_t is the total cross-section and σ_s is the double-differential scattering cross-section. The source and angular flux are functions of six independent variables: a three-dimensional position vector (\vec{r}) a two-dimensional directional vector ($\hat{\Omega}$), and energy (E). The adjoint identity is stated as

$$\langle \Psi^+, H\Psi \rangle = \langle \Psi, H^+\Psi^+ \rangle \quad (2.6)$$

where $\langle \cdot \rangle$ refers to the integration over space, energy, and angle and the adjoint operator H^+ is given by

$$H^+ = -\hat{\Omega} \cdot \nabla + \sigma_t(\vec{r}, E) - \int_0^\infty dE' \int_{4\pi} d\Omega' \sigma_s(\vec{r}, E \rightarrow E', \hat{\Omega} \rightarrow \hat{\Omega}') \quad (2.7)$$

This identity can be used to form the adjoint transport equation.

$$H^+\Psi^+ = q^+ \quad (2.8)$$

Substituting Eq.2.4 and 2.8 into Eq. 2.6, the adjoint identity can also be written as

$$\langle \Psi^+, q \rangle = \langle \Psi, q^+ \rangle \quad (2.9)$$

As mentioned, the solution to the adjoint transport equation will be used as an importance function therefore the thoughtful selection of an adjoint source q^+ is needed.

Consider the equation for detector response, R

$$R = \langle \Psi, \sigma_d \rangle \quad (2.10)$$

where σ_d is a detector response function. If the adjoint source is chosen to be equivalent to the detector response function,

$$q^+ = \sigma_d \quad (2.11)$$

and substituted into Eq. 2.10

$$R = \langle \Psi, q^+ \rangle \quad (2.12)$$

the response has the same form as the right side of Eq. 2.9, therefore the response can also be written as a function of the adjoint solution

$$R = \langle \Psi^+, q \rangle \quad (2.13)$$

This final relation allows us to know the response R for any source q once the adjoint solution Ψ^+ to a quantity of interest is known.

2.4.1 CADIS

The Consistent Adjoint Driven Importance Sampling (CADIS) method is one of the hybrid deterministic/MC VR techniques that uses the adjoint solution as an importance function to formulate VR parameters for MC transport [1]. More specifically, CADIS provides a method for generating a biased source and the weight window lower bounds in a consistent manner. The consistent generation of biasing parameters ensures that particles are born within weight windows, eliminating any loss of efficiency due to particle splitting/rouletting immediately after birth. Recall that the response, or tally, of interest in a transport calculation can be represented in terms of the adjoint flux by Eq. 2.13. To decrease the variance, the CADIS method formulates a biased source distribution that represents the contribution of particles from phase space $(\vec{r}, E, \hat{\Omega})$ to the total detector response, R .

$$\hat{q}(\vec{r}, E, \hat{\Omega}) = \frac{\Psi^+(\vec{r}, E, \hat{\Omega}) q(\vec{r}, E, \hat{\Omega})}{R} \quad (2.14)$$

This essentially is a way to bias the sampling of source particles as a function of their contribution to the total detector response. As previously mentioned, when sampling from a biased distribution, the particle weight

needs to be adjusted such that total weight is conserved in order to eliminate systematic bias.

$$w(\vec{r}, E, \hat{\Omega}) \hat{q}(\vec{r}, E, \hat{\Omega}) = w_0 q(\vec{r}, E, \hat{\Omega}) \quad (2.15)$$

Substituting Eq. 2.14 into Eq. 2.15 and setting w_0 equal to one, the corrected particle weight is given as

$$w(\vec{r}, E, \hat{\Omega}) = \frac{R}{\Psi^+(\vec{r}, E, \hat{\Omega})} \quad (2.16)$$

The width of the weight windows is determined by a parameter defined to be the ratio between upper and lower bounds $\alpha = w_u/w_l$. MCNP uses a default value of 5 for α . The equation for weight window lower bounds is given as

$$w_l(\vec{r}, E, \hat{\Omega}) = \frac{R}{\Psi^+(\vec{r}, E, \hat{\Omega})^{(\frac{\alpha+1}{2})}} \quad (2.17)$$

CADIS is ideally suited to reduce the variance of a detector response in a single target because the source chosen for adjoint transport is the detector response function corresponding to the detector of interest. There are other methods, such as FW-CADIS, that are suited for reducing the variance in multiple targets or even globally.

2.4.2 FW-CADIS

The Forward-Weighted (FW)-CADIS method is another hybrid deterministic/MC VR method. FW-CADIS aims to increase the efficiency of detector responses globally or in multiple localized targets [10]. The goal is to create uniform particle density in the tally regions thereby creating uniform statistical uncertainty in the MC results. This method relies upon a forward deterministic transport solution to weight the source for adjoint deterministic transport. The adjoint solution is then used with the stan-

dard CADIS method to produce source and transport biasing parameters for the forward MC transport simulation.

If the objective is a spatially dependent total response rate, the FW-CADIS adjoint source is formulated as

$$q^+(\vec{r}, E) = \frac{\sigma_d(\vec{r}, E)}{\int_E \phi(\vec{r}, E) \sigma_d(\vec{r}, E) dE} \quad (2.18)$$

where $\sigma_d(\vec{r}, E)$ is the response function. This effectively weights the adjoint source by the inverse of the total forward response which means that in regions with low forward flux, the adjoint flux, and therefore importance, will be high and vice versa. This will result in the overall goal of nearly equal statistical uncertainty in regions of interest.

2.5 Automated Variance Reduction for Multi-physics Analysis

In its essence, SDR analysis is the analysis of a coupled, multi-physics system; the initial neutron irradiation is coupled to the decay photon transport through activation analysis. As discussed in section 2.2.2, the R2S method requires separate MC calculations for the neutron and photon transport. If the MC steps are performed in analog, applying the R2S workflow to full-scale, 3D FES becomes impractical due to the computational effort required to produce accurate space- and energy-dependent fluxes throughout the geometry.

Optimizing the final step, photon transport in the case of SDR analysis, can be done through a straightforward application of the CADIS method to solve for the response at a single detector or the FW-CADIS method if the response is desired in multiple detectors or globally.

Optimizing the initial step of a multi-step process, neutron transport in

the case of SDR, is not as straightforward. The Multi-Step CADIS method described in the next section provides an explanation for this challenge and a method for solving it.

2.5.1 MS-CADIS

The Multi-Step (MS)-CADIS method of VR was developed to optimize the primary radiation transport in a coupled, multi-step process.

Optimizing the initial radiation transport relies upon the use of a function that represents the importance of the particles to the final response of interest, not the response of that individual step [11]. This is challenging because the the final response of interest depends on the subsequent steps of the multi-step process.

MS-CADIS can be applied to any coupled, multi-step process, but when applied to SDR calculations, it aims to increase the efficiency of the neutron transport step using an importance function that captures both the potential of regions to become activated and their potential to produce decay photons that contribute tto the final SDR [11].

The importance function represents the expected contribution from a particle at some point in phase space to the detector response. In the theoretical scenario that every source particle contributes the exact expected value, the detector response can be expressed as the inner product of the importance function, I , and the source distribution, q .

$$R = \langle I(\vec{r}, E), q(\vec{r}, E) \rangle \quad (2.19)$$

MS-CADIS provides a method to calculate an approximation of this importance function where the response is the final response of the multi-step process. In the case of an R2S calculation, the final response is the SDR

caused by the decay photons. The SDR is defined as

$$\text{SDR} = \langle \sigma_d(\vec{r}, E_\gamma), \phi_\gamma(\vec{r}, E_\gamma) \rangle \quad (2.20)$$

where σ_d is the flux-to-dose-rate conversion factor at the position of the detector and ϕ_γ is photon flux. Following the CADIS method, the adjoint photon source is chosen to be σ_d , so the equation for SDR becomes

$$\text{SDR} = \langle q_\gamma^+(\vec{r}, E_\gamma), \phi_\gamma(\vec{r}, E_\gamma) \rangle \quad (2.21)$$

From the adjoint identity, Eq. 2.9, the SDR can also be written as

$$\text{SDR} = \langle q_\gamma(\vec{r}, E_\gamma), \phi_\gamma^+(\vec{r}, E_\gamma) \rangle \quad (2.22)$$

which has the same form as Eq. 2.19. Therefore, it can be seen that the adjoint flux, ϕ_γ^+ , is the importance function.

Because the final goal is to formulate a function that represents the importance of neutrons the final SDR, the neutron response is set equal to the photon response.

$$\text{SDR} = \langle q_n^+(\vec{r}, E_n), \phi_n(\vec{r}, E_n) \rangle = \langle q_n(\vec{r}, E_n), \phi_n^+(\vec{r}, E_n) \rangle \quad (2.23)$$

It can be seen that the far right side of Eq. 2.23 also has the same form as Eq. 2.19 which means that the adjoint neutron flux, ϕ_n^+ , serves as the importance function used to optimize the neutron transport.

Combining equations 2.22 and 2.23, gives the relationship between the neutron and photon responses.

$$\langle q_n^+(\vec{r}, E_n), \phi_n(\vec{r}, E_n) \rangle = \langle q_\gamma(\vec{r}, E_\gamma), \phi_\gamma^+(\vec{r}, E_\gamma) \rangle \quad (2.24)$$

To generate the adjoint neutron flux, an adjoint neutron source, q_n^+ , first needs to be formulated. This requires Eq. 2.24 and another equation

relating the photon source, q_γ , to the neutron flux, ϕ_n . The solution method for the adjoint neutron source, q_n^+ , will be discussed in the next section.

2.5.2 GT-CADIS

The Groupwise Transmutation (GT)-CADIS method is an implementation of MS-CADIS solely for SDR analysis. It provides a solution to the adjoint neutron source, q_n^+ , by calculating a coupling term that relates the neutron flux to the photon source [14].

Neutron activation is the cause of the photon decay source so the photon source at a single point can be expressed as a non-linear function of ϕ_n

$$q_\gamma(E_\gamma) = \int_{E_n} f(\phi_n) dE_n \quad (2.25)$$

This function can not be linearized for arbitrary transmutation networks and irradiation scenarios, but a linear relationship can be formulated when a set of criteria, known as the Single Neutron Interaction Low Burnup (SNILB) criteria, are met. When met, a solution for the coupling term, $T(\vec{r}, E_n, E_\gamma)$, which approximates the transmutation process and is defined by the following equation

$$q_\gamma(\vec{r}, E_\gamma) = \int_{E_n} T(\vec{r}, E_n, E_\gamma) \phi_n(\vec{r}, E_n) dE_n \quad (2.26)$$

can be found. Eq. 2.26 can then be substituted into Eq. 2.24 in order to solve for the adjoint neutron source as shown below

$$q_n^+(\vec{r}, E_n) = \int_{E_p} T(\vec{r}, E_n, E_p) \phi_p^+(\vec{r}, E_p) dE_p \quad (2.27)$$

To calculate T , a series of single energy group neutron irradiations is performed on each material in the geometry. The photon sources that are

a function of each neutron energy group can then be used to calculate T via Eq. 2.26.

It has been shown that for typical FES spectra, materials, and irradiation scenarios, the SNILB criteria are met; therefore, GT-CADIS provides a solution for T , and therefore the adjoint neutron source needed to optimize the neutron transport for SDR analysis of FES.

2.6 Moving Geometries and Sources

2.6.1 MCNP6 Moving Objects Capability

Historically, Monte Carlo analysis of moving systems was performed using a series of separate simulations with different input files that contained step-wise changes of the geometry configuration. The new moving object capability that will be available in a future version of MCNP6 allows for the motion of objects, sources, and delayed particles during a single simulation [12], [13]. This capability allows for rigid body transformations of objects including rectilinear translations and curvilinear translations and rotations. The objects can move with constant velocity, constant acceleration, or be relocated. Object kinetics are not treated, however, so the user must use caution and supply transformations that will not cause objects to overlap. This capability is currently applicable to MCNP's native geometry format, constructive solid geometry (CSG), and is not available for mesh-based geometries.

Sources can be assigned to moving objects, therefore can move with the same dynamics as other objects in the problem. This capability also allows for the treatment of secondary particles emitted by objects in motion. This treatment is only approximate because the geometry is fixed during the transport of source or delayed particles. This is a valid approximation due to the assumption that the geometry movement is orders of magnitude slower than particle transport.

During the MCNP simulation, source particles are tracked through the geometry from the time of emission to termination. If any of the source particle's interactions result in the creation of a prompt or delayed secondary particle, that information is stored. After the source particle has terminated, any stored secondary particles are retrieved and transported. In the case of delayed particles emitted from moving objects, the location, direction, energy, and time are stored at the time of fission or activation and then at the time of emission, the geometry configuration is updated to provide the correct location and orientation of the delayed particle.

2.6.2 MCR2S with Geometry Movement

The Mesh Coupled implementation of R2S (MCR2S), developed by the Culham Science Center, was updated to allow geometry components to change location after shutdown [?]. This capability was developed to facilitate SDR calculation during maintenance and intervention activities. MCR2S relies on MCNP for both neutron and photon transport steps and FISPACT for the activation calculations. It allows multiple components to be moved to different locations prior to the photon transport step.

These geometry translations occur by creating a copy of the components that will move. Transform cards are applied to the copies. The original components remain in their original locations and their material is changed to vacuum. Any source particle that starts in one of the components that moves after shutdown is automatically translated to the correct location.

The requirement that both the original component (set as void) and its transformed copy are present during the photon transport step means that there can be no overlap between the parts which could be problematic for small transformations.

3 EXPERIMENT

3.1 Demonstration of GT-CADIS

GT-CADIS has proven to be an effective method for optimizing the neutron transport step of SDR analysis in static FES when the SNILB criteria are met [14]. As it stands, this method will not provide appropriate VR parameters for the cases where activated components are moving after shutdown. The following experiment will demonstrate the need for a time-integrated adjoint photon solution in order to provide useful VR parameters for dynamic systems.

3.1.1 Problem Description

The source, geometry, and materials chosen for this demonstration are a simplified representation of those found in fusion energy devices. A planar view of the geometry is shown in Fig. 3.1. It is composed of a chamber of Stainless Steel 316 (SS-316) with a central cavity measuring 2m x 2m x 2 m. The walls are 2 m thick. The chamber is surrounded by air and there is helium in the central cavity. A CAD model of this geometry was built and the components tagged with material names using Trelis [19]. A neutron source was placed in the central cavity; it was sampled uniformly in space and within the energy interval of 13.8-14.2 MeV. The SDR is measured with a detector after a single pulse irradiation of 10^5 s and decay period of 10^5 s. The detector is a sphere, 10 cm in radius, located 2 m in the positive x-direction away from the outer wall of the steel chamber. The detector material was chosen to be the same as that used in a previous GT-CADIS experiment (52.34 at. % H-1, 47.66 at. % C-12) [14].

First, the R2S workflow was performed with analog (except for implicit capture) MC neutron and photon transport steps. Then, the GT-CADIS



Figure 3.1: Planar view of the geometry. Steel chamber with 2 m thick and central cavity measuring 2 m x 2 m x 2 m. The central cavity is filled with helium and chamber is surrounded by air. A SDR detector is located 2 m in the x-direction from the chamber.

method was used to generate VR parameters to optimize the neutron transport step.

3.1.2 Analog R2S

The main steps of the R2S workflow are as follows:

1. MC Neutron Transport
2. Activation Analysis
3. MC Photon Transport

MCNP5 [3] was chosen as the MC code and ALARA [20] as the activation code.

Need
to label
this
figure

First, a DAGMCNP5 [18] simulation with 10^7 histories was run using the CAD geometry generated by Trelis and an input file that contained a Cartesian mesh tally over the entire geometry to score neutron flux. A 175 group VITAMIN-J energy structure [22] was applied to the mesh tally in order to achieve both a spatial and energy-wise distribution of the neutron flux. The resulting neutron flux and relative error for the 13.8-14.2 MeV energy group are shown in Fig. ??.

A script in PyNE's R2S module was used to construct the ALARA input files using the neutron flux mesh. ALARA was run using FENDL2.0 nuclear data [24]. PyNE R2S was used again to generate a mesh-based photon source from the ALARA output. The photon source is shown in Fig. 3.3.

3.1.3 GT-CADIS

To optimize the neutron transport step of R2S, the GT-CADIS method was used to generate a biased source and weight windows. The main steps of the GT-CADIS method are as follows:

1. Deterministic adjoint photon transport
2. Calculation of the GT-CADIS adjoint neutron source
3. Deterministic adjoint neutron transport
4. Generation of biased source and weight windows from adjoint neutron flux

The deterministic code PARTISN [17] was chosen to perform the adjoint transport steps. The source used for adjoint photon transport was a 42 energy group VITAMIN-J discretization of the ICRP-74 flux-to-dose conversion factors [21]. The CAD geometry was discretized onto a Cartesian mesh that exactly conformed to the geometry boundaries so no material

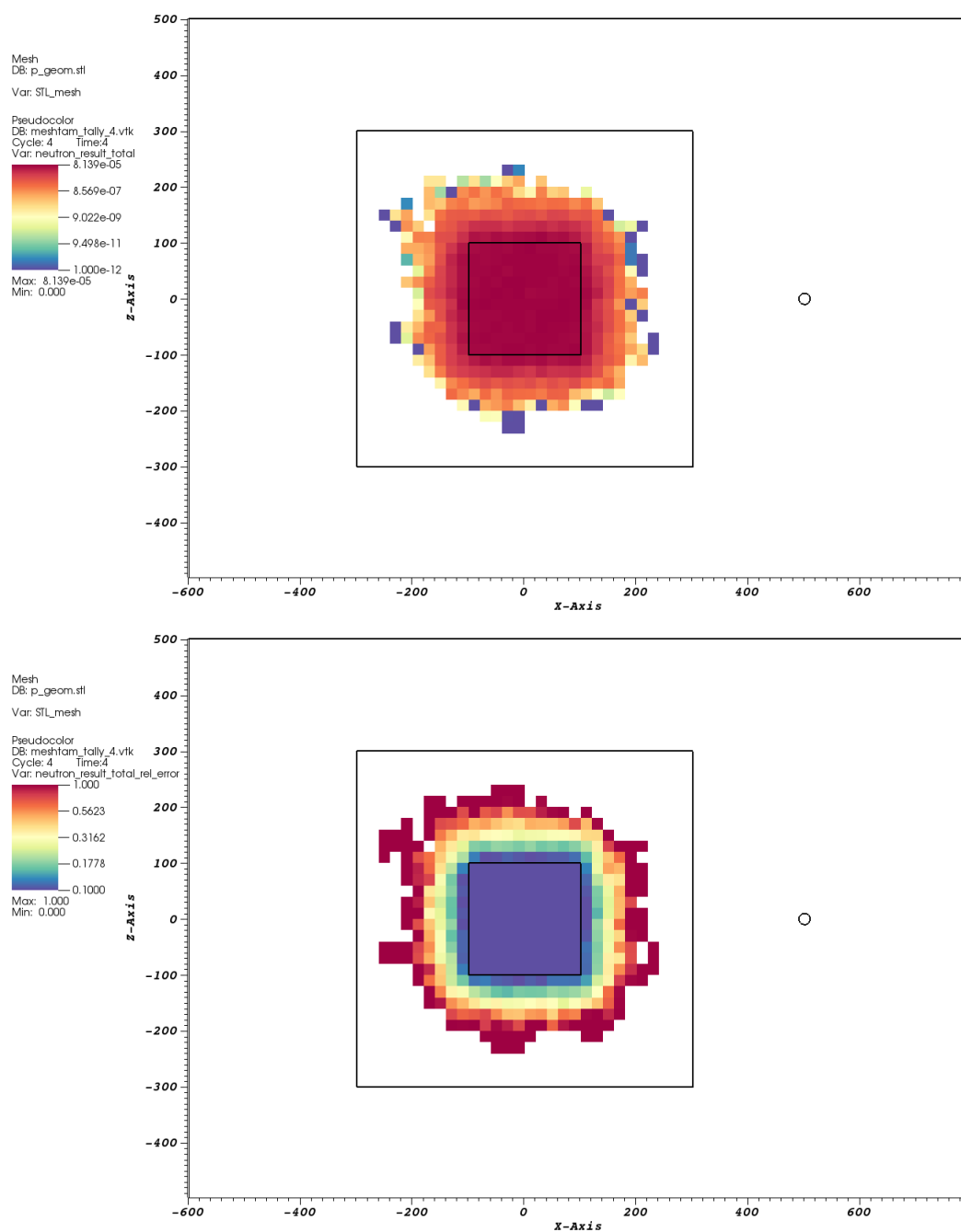


Figure 3.2: Neutron flux (top) and relative error (bottom) resulting from analog MC simulation.

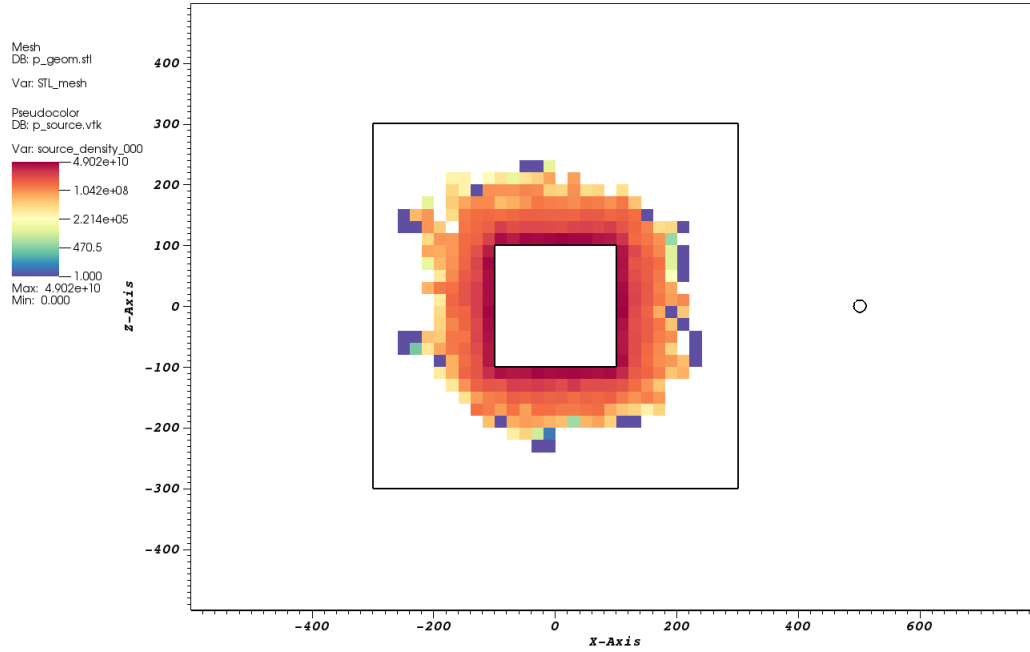


Figure 3.3: Photon source generated by ALARA activation calculation using the analog MC neutron transport result.

mixing was required. The resulting adjoint photon flux mesh is shown in Fig. 3.4.

Next, the coupling term T was calculated for each material: SS316, air, and helium. This was done by performing separate 10^5 s irradiation and 10^5 s decay ALARA simulations for each of 175 neutron energy groups in each of the materials to obtain the photon source in each photon energy group as a function of the neutron flux in each neutron energy group. T was then calculated using Eq. 2.26.

This T was combined with the adjoint photon flux to generate the GT-CADIS adjoint neutron source via Eq. 2.27. PARTISN was run again using this adjoint neutron source and the resulting adjoint neutron flux for the 13.8-14.2 MeV energy group is shown in Fig. 3.5.

This adjoint neutron flux functions as an importance map of neutrons

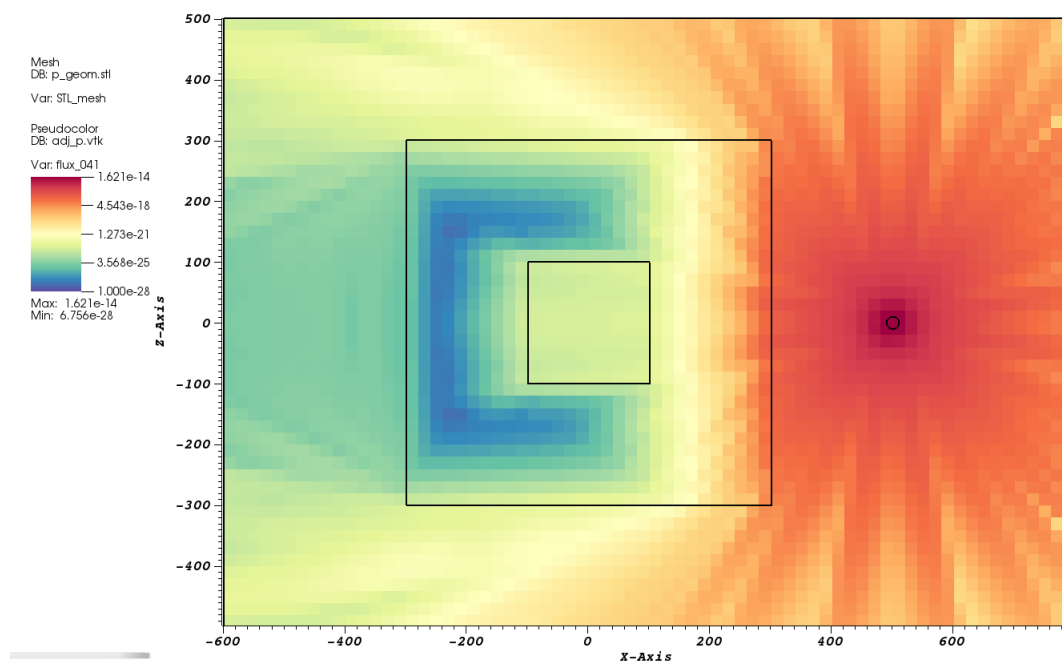


Figure 3.4: Adjoint photon flux used to generate adjoint neutron source according to the GT-CADIS method.

to the final SDR. In the region of the steel chamber near the detector, there is a high flux, therefore neutrons in this region have a high importance to the SDR. In contrast, there is a low flux in the regions on the far side of the detector. Neutrons in this region are less likely to activate materials that will then produce decay photons that contribute to the SDR.

The adjoint neutron flux were then used to generate the biased source and weight windows via the CADIS method. These are seen in Fig. 3.6 and Fig. 3.7.

The biased source and weight window files were used to optimize the neutron transport step of R2S. A DAGMCNP5 simulation with 10^7 histories was performed using these VR parameters and the resulting neutron flux and relative error are shown in Fig. 3.8.

ALARA was run using the neutron flux and the same irradiation and

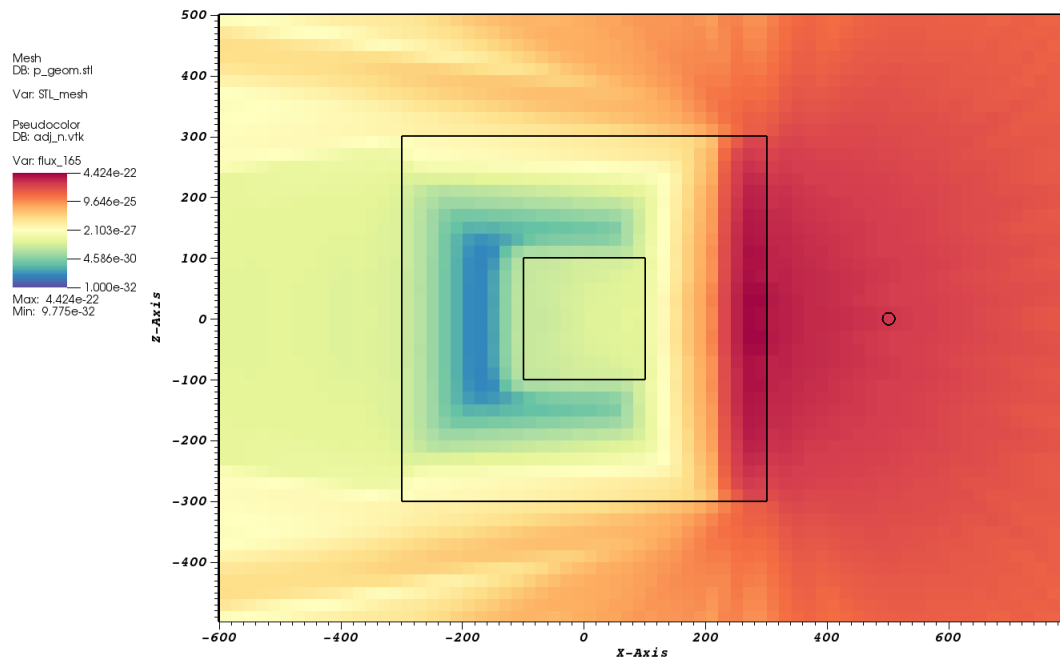


Figure 3.5: Adjoint neutron flux used to generate the biased source and weight windows according to the GT-CADIS method.

decay scenario used to calculate T (10^5 s irradiation, 10^5 s decay). The photon source distribution generated is shown in Fig. 3.9

3.2 Limitations of GT-CADIS for Moving Systems

Comparing the neutron flux and relative error obtained by the analog MC transport in Fig. 3.2 and that obtained using the GT-CADIS method in Fig. 3.8, it is clear to see that given the same number of histories, the GT-CADIS method not only reduces the error in regions of the steel chamber that are important to the SDR, but allows a solution to be calculated in the detector region.

Show these figures on the same page so they are

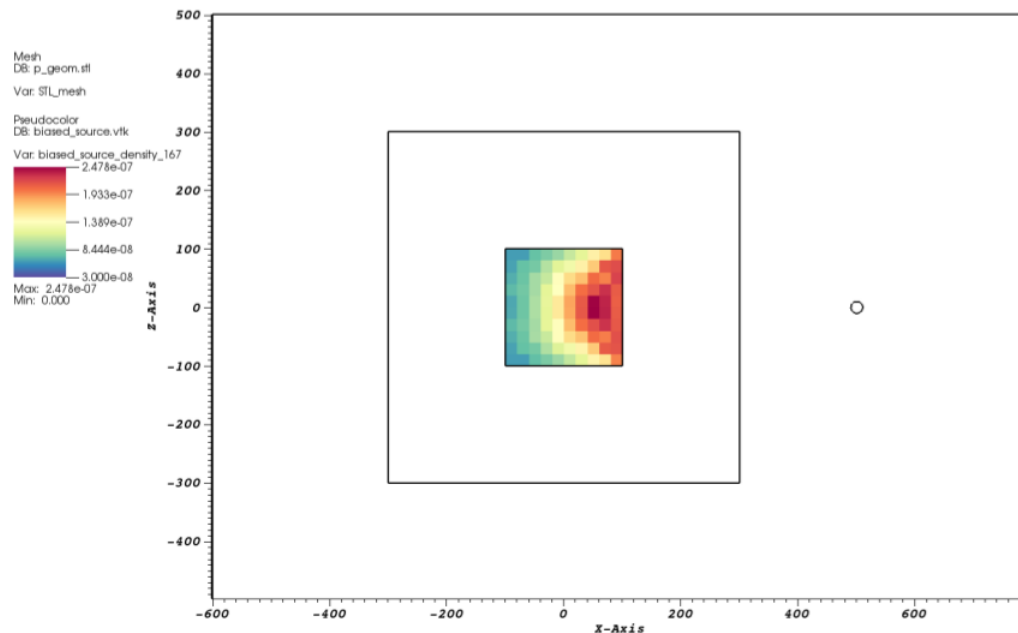


Figure 3.6: Biased neutron source generated with GT-CADIS method.

Now, consider if the steel chamber was not a monolithic block, and instead made of modular components that can move after shutdown, during the photon decay process. For example, a component of the chamber originally located on the far side of the detector moves to a location near the detector as shown in Fig. 3.10. The photons produced in the activated, moving component become more likely to contribute to the SDR as the component moves closer to the detector. This also means that the neutrons in this region are important because it is the neutron irradiation that results in photon emission.

Highlighting the region of the moving component in the adjoint neutron flux map produced by GT-CADIS, Fig. 3.11, it can be seen that this is no longer a valid importance map of the neutrons to the final SDR. There is a low flux, therefore low importance in the moving component that will

Label
orig lo-
cation,
final
locat-
ion,
de-
tector.
Make
central
cavity
white

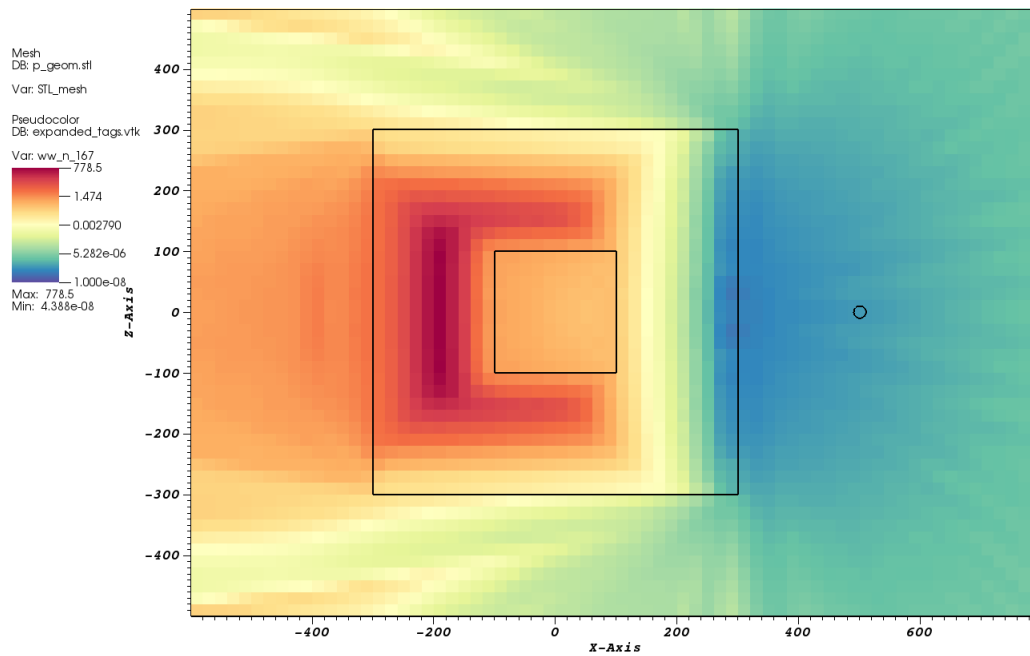


Figure 3.7: Weight window mesh generated with GT-CADIS method.

eventually be positioned near the detector. Because this adjoint neutron flux is used to generate source and transport biasing parameters, neutrons will be steered away from interactions in this component, increasing the uncertainty in a region that will ultimately be important to the SDR.

Are these two statements strong enough? This is the whole point of the work.

Arrange figures so they appear

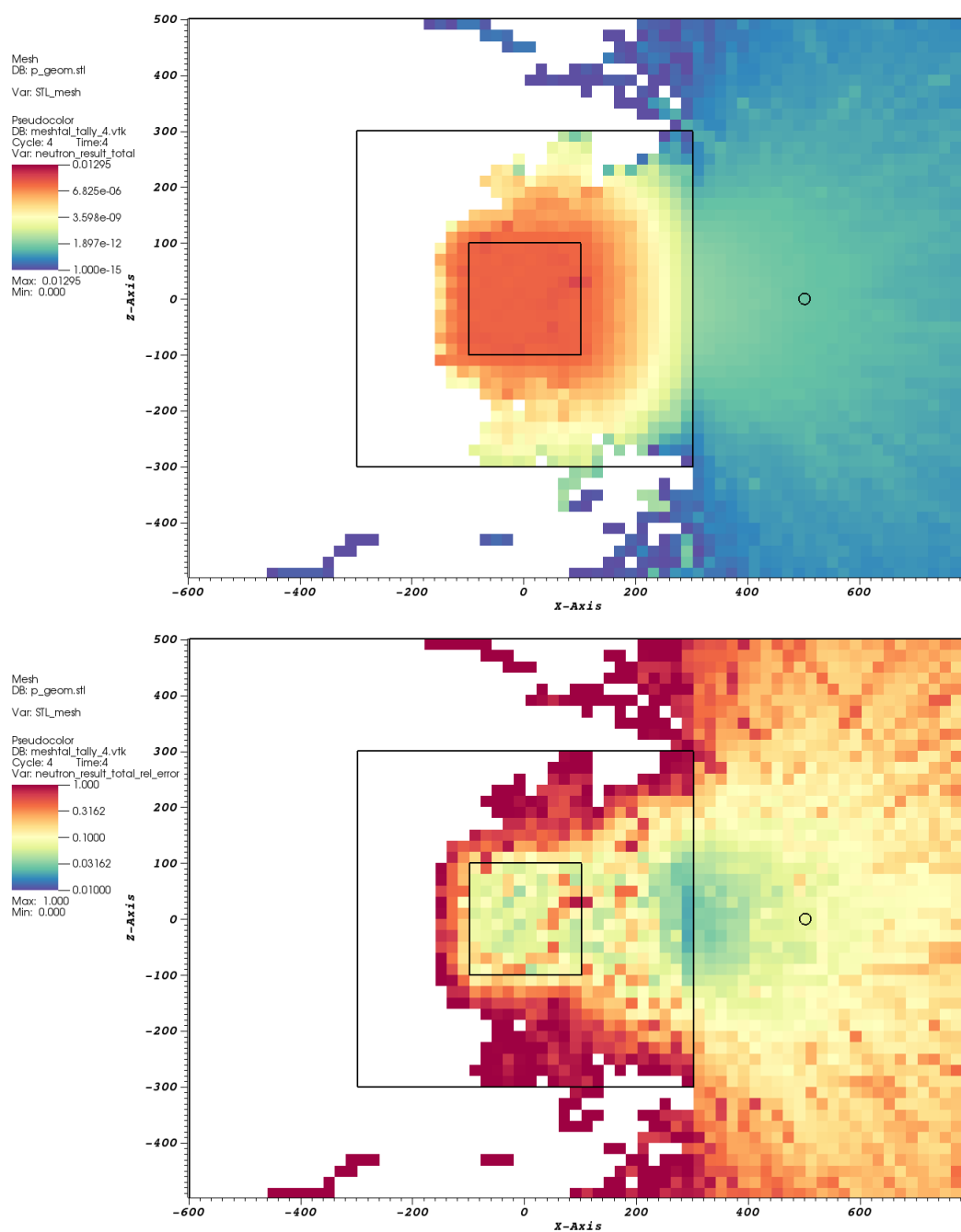


Figure 3.8: Neutron flux and relative error resulting from MC simulation using GT-CADIS biased source and weight window mesh.

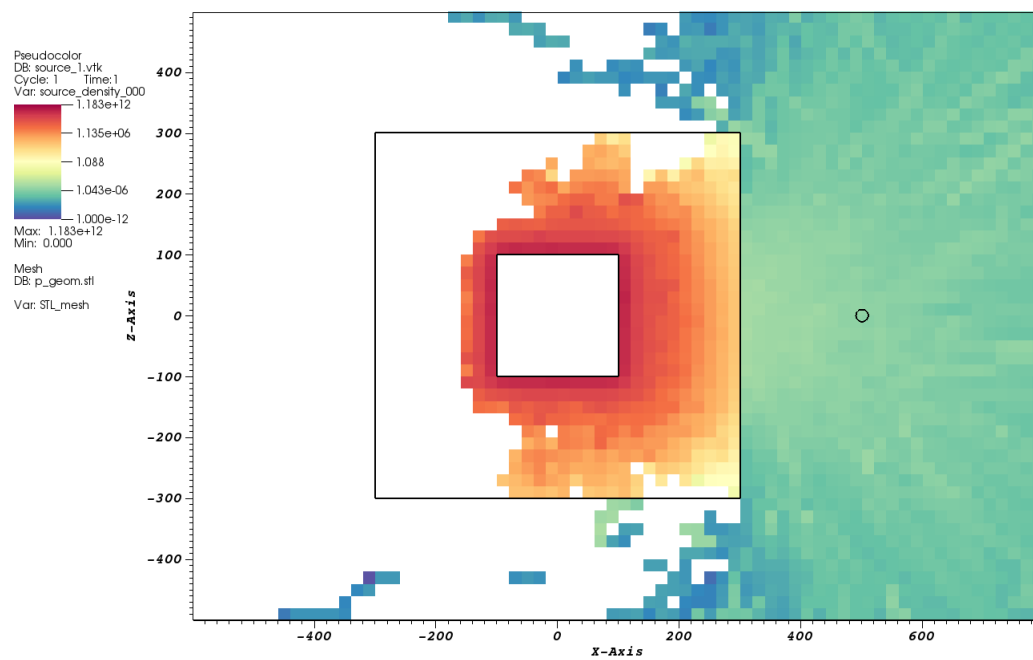


Figure 3.9: Photon source generated after ALARA activation calculation using the GT-CADIS optimized neutron transport result.

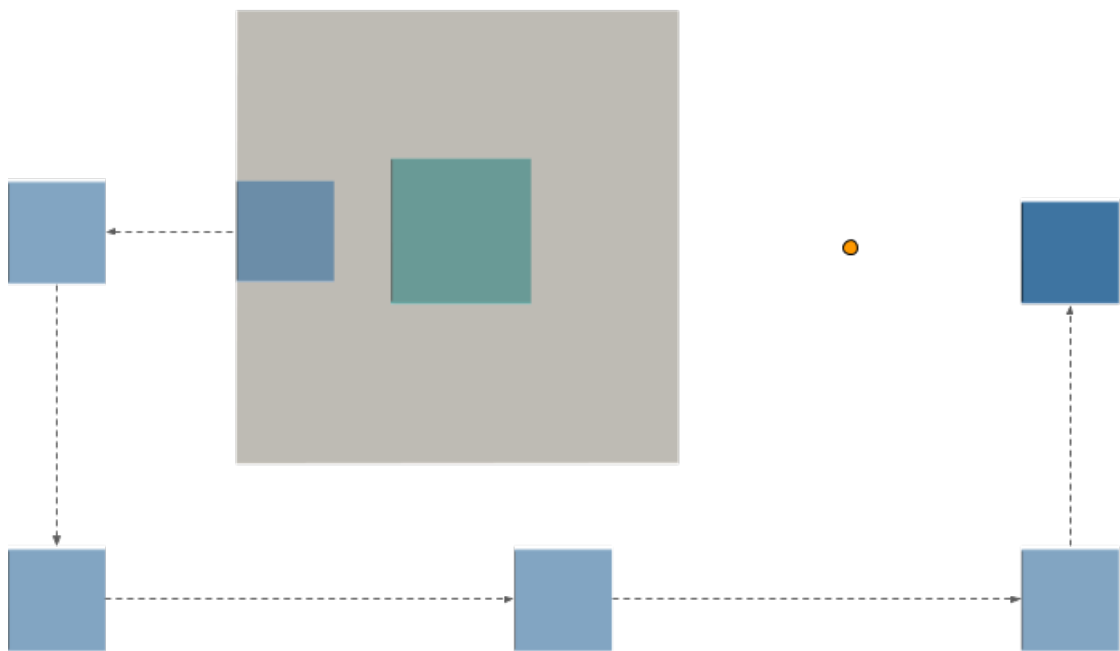


Figure 3.10: Path of activated component moving from the far side of the SDR detector to position next to it.

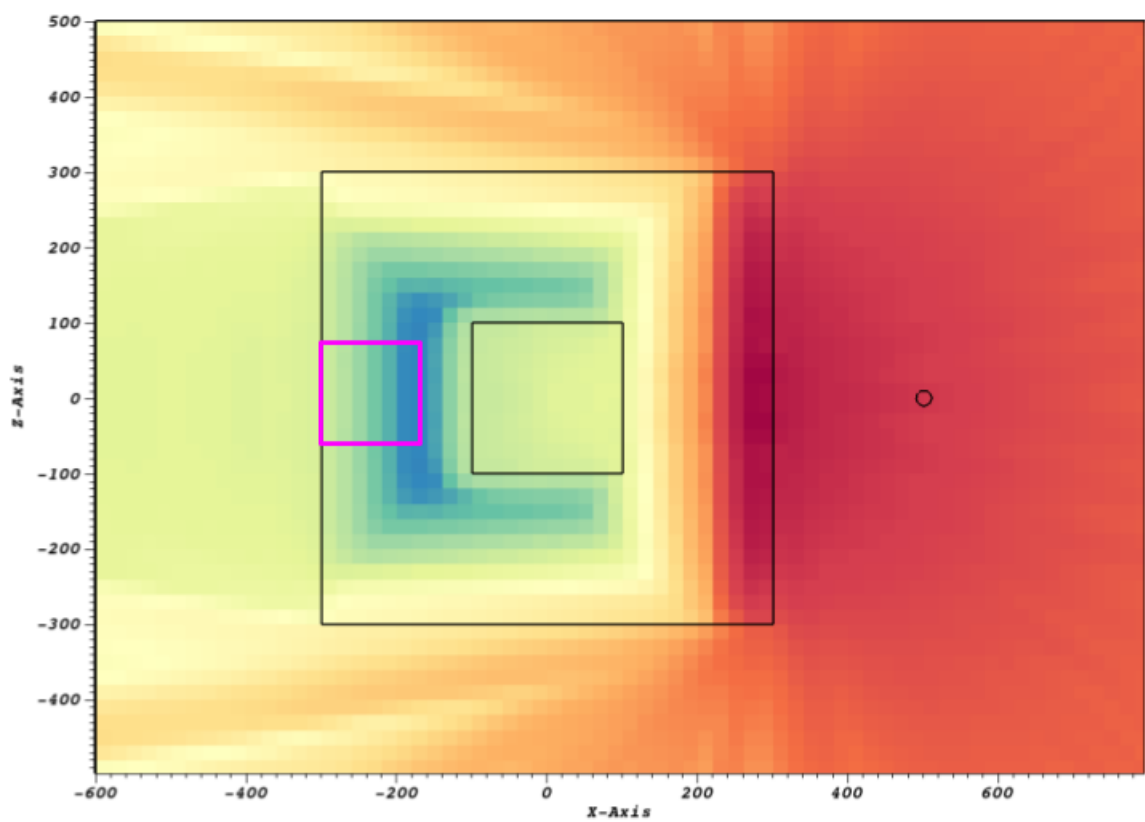


Figure 3.11: Adjoint neutron flux map with region of moving component highlighted.

4 VARIANCE REDUCTION FOR TIME-INTEGRATED MULTIPHYSICS ANALYSIS

The Multi-Step Consistent Adjoint Weighted Importance Sampling (MS-CADIS) method of variance reduction was developed to optimize the primary radiation transport in a coupled, multi-step process. The first implementation of this method was applied to the coupled neutron activation-photon decay process that occurs in FES. In its current form, MS-CADIS is only applicable to static systems where the geometry remains unchanged in all steps of the multi-step process.

This chapter will first discuss MS-CADIS outside of the context of SDR analysis. Next, a time-integrated solution to the adjoint of the physical process occurring during geometry movement will be derived. Finally, this time-integrated solution will be applied to the GT-CADIS method to form the Time-integrated (T)GT-CADIS adjoint neutron source that will ultimately be used to optimize the neutron transport step of SDR analysis.

4.1 Generalized MS-CADIS Method

In the current literature, MS-CADIS is primarily discussed as it applies to SDR analysis [11]. In actuality, MS-CADIS can be applied to any multi-step process in which the primary radiation transport is coupled to a secondary physical process. The addition of time integration to this methodology can also be applied to any coupled multi-physics process. For this reason, it is prudent to discuss MS-CADIS in a more generalized manner.

To describe the system of coupled, multi-physics, the operator notation of the Boltzmann transport equation

$$H\phi = q \tag{4.1}$$

where H operates on the particle flux ϕ and q is a source of particles, will be used to represent the initial radiation transport and an equation of the same form

$$L\Psi = b \quad (4.2)$$

where L operates on some function Ψ and b is a source term, will be used to describe a generic secondary physics. The adjoint identity for the neutral particle transport equation was given in Eq. 2.6. This identity is valid for an arbitrary adjoint source function [15], therefore the secondary physics has an adjoint identity of the same form

$$\begin{aligned} \langle \Psi^+, L\Psi \rangle &= \langle \Psi, L^+\Psi^+ \rangle \\ \langle \Psi^+, b \rangle &= \langle \Psi, b^+ \rangle \end{aligned} \quad (4.3)$$

where $\langle \cdot \rangle$ signifies the integration over all dependent variables. Assume this is a two-step system and the ultimate quantity of interest is the response of the secondary physics which takes the form

$$R_{\text{final}} = \langle \sigma_b, \Psi \rangle \quad (4.4)$$

where σ_b is a response function. According to the CADIS method, if the adjoint source is set equal to the detector response function, the adjoint solution forms the importance function. Substituting the adjoint source, b^+ , into Eq. 4.4 yields the following

$$R_{\text{final}} = \langle \Psi, b^+ \rangle \quad (4.5)$$

Not
sure if
this is
clear.

Combining Eq. 4.5 with the adjoint identity yields

$$R_{\text{final}} = \langle \Psi^+, b \rangle \quad (4.6)$$

For a coupled, multi-step process, the MS-CADIS method constrains the primary adjoint response such that it is equal to the final response of

the system as shown below

$$R_{\text{final}} = \langle \phi, q^+ \rangle = \langle \phi^+, q \rangle \quad (4.7)$$

Ultimately, the goal is to find a solution to the adjoint primary radiation transport to use as an importance function for the forward calculation. Therefore, a source for the adjoint radiation transport is needed. Equating the adjoint response equations in Eq. 4.7 and 4.6, yields the following expression.

$$\langle \phi, q^+ \rangle = \langle \Psi^+, b \rangle \quad (4.8)$$

In a practical scenario, the forward source of radiation (e.g. neutron source resulting from D-T fusion) will be known. The adjoint source of secondary physics is chosen to be the response function for the detector of interest (e.g. flux-to-dose conversion factors). Given that these sources are known, both solutions, ϕ and Ψ^+ , can be found through transport operations. The source of the forward secondary, b , and adjoint primary physics, q^+ , are both unknown, therefore a second equation is needed. This is a coupled, multi-physics system where the source of the secondary physics is a response of the primary radiation transport therefore the two processes can be related by the following definition

$$b = \langle \sigma_c, \phi \rangle \quad (4.9)$$

where σ_c is a function that couples the primary radiation transport to the secondary physics.

Consider the process of neutron-induced prompt photon production. In this case, the function, σ_c , is the neutron-gamma production cross section, $\sigma_{n,\gamma}$. The primary focus of SDR analysis is the process of neutron-induced delayed gamma production. GT-CADIS provides a method for calculating σ_c when certain conditions (known as SNILB) hold true. In

this case, the coupling term, T , is an approximation of the transmutation process [14]. As long as there is a solution for σ_c , the function that couples the primary and secondary physics together, there also exists a solution for the adjoint radiation transport source. This can be discovered by substituting Eq. 4.9 into Eq. 4.8 and solving for q^+ .

$$q^+ = \langle \sigma_c, \Psi^+ \rangle \quad (4.10)$$

4.2 Time-integrated MS-CADIS

If the configuration of the geometry is changing over time during the secondary physics, it will affect the construction of the adjoint radiation transport source, q^+ . The solutions to both forward and adjoint transport will be calculated in discrete volume elements. There is a solution to the adjoint secondary physics at each position and each time.

- $\Psi^+(\vec{r}_v(t), t)$ Adjoint flux in volume element v at time t
- $\vec{r}_v(t)$ Position of volume element v at time t

To solve for the adjoint radiation source in each volume element, q_v^+ , the time-dependent solutions of the adjoint secondary physics are combined by integrating over time.

$$q_v^+ = \int_t \Psi^+(\vec{r}_v(t), t) \sigma_{c,v}(t) dt \quad (4.11)$$

This time-integrated source term is then used for adjoint radiation transport to obtain ϕ_v^+ .

4.3 Time-integrated GT-CADIS

GT-CADIS is an implementation of MS-CADIS that is specific to SDR analysis. It provides a method to calculate a coupling term, T , that relates the neutron flux to the photon source. T is then used to solve for the adjoint neutron source as shown in Eq. 2.27. If the geometry configuration changes after shutdown, the time-integrated MS-CADIS methodology shown in the previous section can be applied to the GT-CADIS adjoint neutron source. Adjoint photon transport at each time step during geometry movement, t , will provide the adjoint flux of photons of energy E_γ , in volume element v , at time t , $\phi_\gamma^+(\vec{r}_v(t), E_\gamma, t)$

$$q_{n,v}^+(E_n) = \int_t \int_{E_\gamma} T_v(E_n, E_\gamma, t) \phi_\gamma^+(\vec{r}_v(t), E_\gamma, t) dE_\gamma dt \quad (4.12)$$

$T_v(E_n, E_\gamma, t)$ is the T value of the material in volume element v , at time t . For many practical problems, T will not change over the course of geometry movement because the time constants of decay and geometry motion are very different. The motion of components occurs over a very short period of time relative to photon decay. Discretizing the energy spectrum into groups, the coupling term that relates the irradiation of the material in volume element v , by a flux of neutrons in energy group g , to the corresponding source of photons in energy group h , is given by

$$T_{v,g,h} = \frac{q_{\gamma,v,h}(\phi_{n,v,g})}{\phi_{n,v,g}} \quad (4.13)$$

Using this groupwise calculation of T , the integral in Eq. 4.12 can be estimated by the sum

$$q_{n,v,g}^+ = \sum_{t_{\text{mov}}} \left(\sum_h T_{v,g,h} \phi_{\gamma,v,h,t_{\text{mov}}}^+ \right) \quad (4.14)$$

where t_{mov} is a time step after shutdown that corresponds to a change in geometry configuration and $\phi_{\gamma, v, h, t_{\text{mov}}}^+$ is the adjoint flux of photons in energy group h , in volume element v , at that time step.

5 PROPOSAL

As demonstrated by the experiment in Chapter 3, the VR parameters generated by the GT-CADIS method are insufficient for optimizing the neutron transport step of SDR analysis in cases that involve the movement of activated components after shutdown. This chapter will first discuss the progress towards CAD geometry movement in radiation transport calculations. Then, an updated R2S workflow that accounts for the movement of activated geometry components after shutdown will be introduced. Next, the implementation details of the time-integrated TGT-CADIS adjoint neutron source derived in chapter 4 are discussed. The propagation of error in SDR analysis and some practical considerations for using these methods will also be addressed. Finally, a demonstration of these methods and a summary of goals to accomplish will be given.

5.1 Progress: DAGMC Simulations with Geometry Transformations

There are various scenarios that involve the motion of geometry components during a radiation transport simulation. One example is the movement of activated components of a fusion energy device during a maintenance operation. This section will discuss the progress of 1) a tool to generate different geometry positions based on an original configuration and 2) an update to DAGMCNP that transforms the geometry based on values given in the MCNP input file. Both have application to this thesis work but are also general purpose tools for any calculation in which the geometry configuration needs to be changed.

5.1.1 Production of Stepwise Geometry Files

A tool has been developed to generate CAD geometry files that capture the movement of components over time based on user-supplied motion vectors or relocation values.

First, a geometry file of the model in its original configuration is created. The geometry components are tagged with transformation numbers that correspond to a motion vector or relocation transform. The tool loads the original geometry and a file containing the transformations. If a motion vector is supplied, a total length of time and a desired number of time steps must also be given. The motion can then be divided into step-wise transformations. The position of the components is updated according to these transformations and a new geometry file is produced for each time step. This tool only handles rigid-body transformations; no geometric deformations or scaling. It also does not handle kinetics, so the user must be cautious to not cause any overlap of components during the geometry movement.

The new geometry files that contain stepwise changes of the geometry configuration can be used as input for transport calculations to determine the response at each time step.

5.1.2 DAGMCNP Geometry Transformations

The ability to read transformation (TRn) cards from the MCNP input file and update the position of the CAD geometry accordingly has been added to DAGMCNP. This capability relies upon the same tagging of components in the CAD geometry file discussed in the previous section. The transformation found in the MCNP input file will be applied to any geometry component that is tagged with the number on the TR card.

If using this capability to perform stepwise radiation transport calculations over time, the user would create one MCNP input file per time

step. Each input file should contain the TR cards necessary to update the position of each component to its new location for that time step. During a DAGMCNP simulation, the geometry is loaded, the MCNP input file is read, the geometry position is updated, and then transport is performed.

5.2 Implementation Plan: Time-integrated SDR Analysis

This section introduces a plan to generate fully optimized, time-integrated SDR maps.

5.2.1 Time-integrated R2S

To produce time-integrated SDR maps, the first two steps of the R2S workflow remain unchanged. The only difference is that multiple photon transport calculations need to be performed; one in the geometry's original configuration and then one for each of N time steps of geometry movement. N photon transport calculations need to be performed at each time step of geometry movement. The main steps of time-integrated (T)R2S are listed below and a full implementation flowchart is given in Fig. 5.1.

1. MC neutron transport simulation on geometry at time step $t_{\text{mov}} = 0$
2. ALARA activation analysis
3. MC photon transport simulations on geometry at each time step $t_{\text{mov}} = 0..N$

A tetrahedral mesh that conforms to the original geometry configuration at $t_{\text{mov}} = 0$ is used as a tally to score the neutron flux. This mesh is tagged with the geometry transformations that will occur after shutdown. The tetrahedral mesh neutron flux tally along with an irradiation and

Change to time-dependent? Time-integrated gives the impression that the SDR at each time step will be averaged together to give a total dose during the movement. What

decay scenario of interest are given as input to the PyNE R2S script to generate ALARA input files. ALARA produces photon source files for each decay time of interest. These ALARA photon source files are converted to tetrahedral mesh based sources by another PyNE R2S script.

Because all source mesh files generated will reflect the original position of the geometry, they, along with the DAGMC geometry files, need to be transformed to the correct locations for each t_{mov} with the DAGMC transform tool. The transformed sources and geometries can then be used as input for the MC photon transport simulations to calculate the SDR at each time step during geometry movement.

5.2.2 Generation of the TGT-CADIS Variance Reduction Parameters

This section discusses the implementation of the time-integrated (T)GT-CADIS adjoint neutron source derived in Chapter 4. First, a CAD model of the geometry in its original position, that during device operation time, is created. This geometry is tagged with transformation numbers corresponding to the stepwise movements that together construct a path from original to final location. The DAGMC transformation tool discussed in section 5.1 is used to apply the transformations and create HDF5 mesh files of the geometry at each time step. A tetrahedral mesh file that conforms to the geometry in its original configuration is also created. This mesh file is tagged with the same transformations as the CAD geometry so that a mesh file is also generated for each time step.

The geometry file at each time step along with the adjoint photon source (the flux-to-dose conversion factors) are given as input into a script that generates a Partisn input file. Deterministic adjoint photon transport is carried out and a Partisn output of the resulting adjoint photon flux in each photon energy group, h , is returned. This Partisn output is converted to an HDF5 Cartesian (voxel) mesh file through a PyNE conversion method.

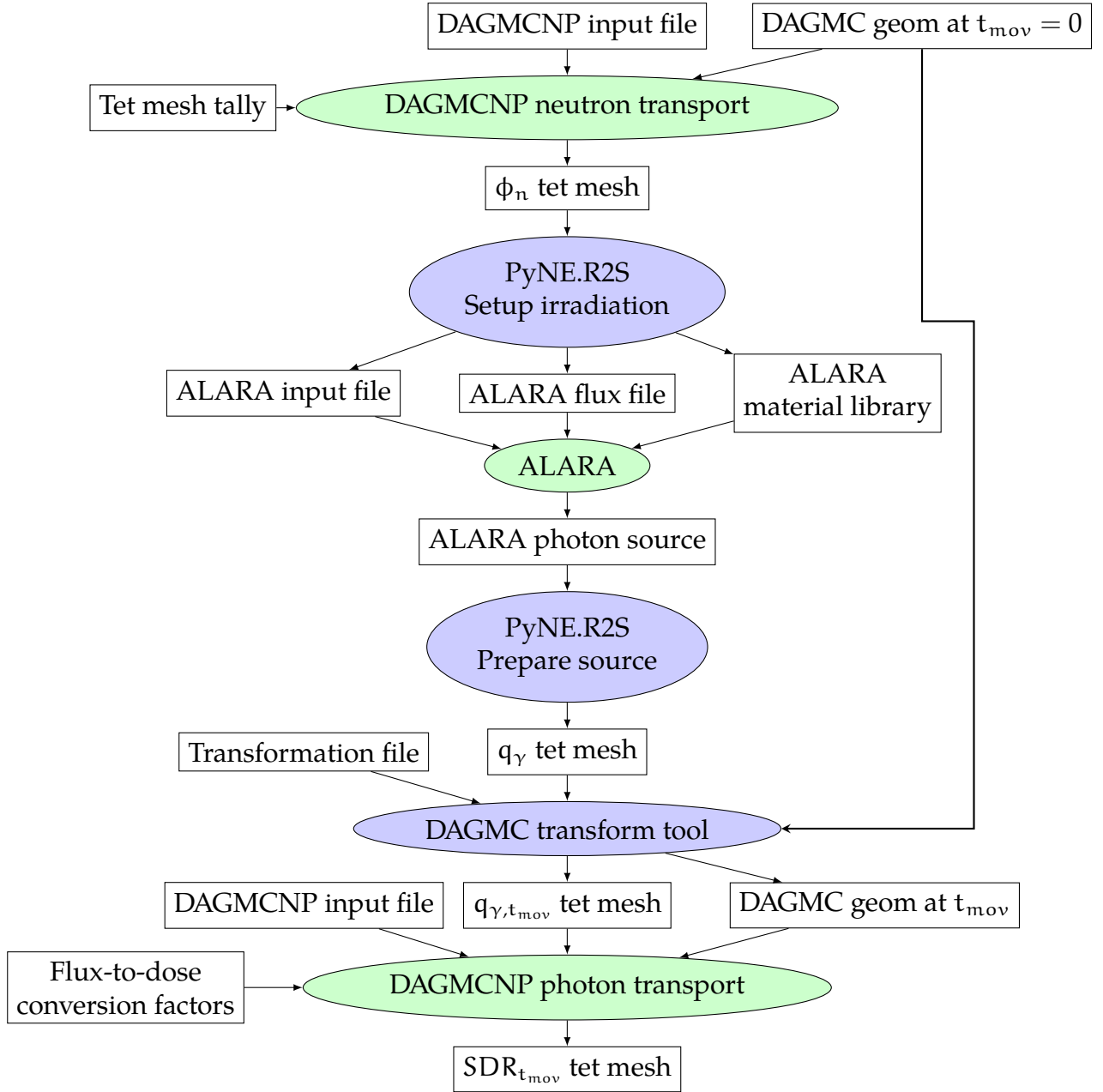


Figure 5.1: Time-integrated R2S (TR2S) workflow for calculating the SDR at each time step of geometry movement after shutdown, t_{mov} . Scripts are shown in blue ovals, physics codes in green ovals, and files in white rectangles.

Because we ultimately need to combine the contribution from each time step in each volume element, the adjoint photon flux voxel mesh is mapped onto the tetrahedral mesh of the geometry at that same time step. Each tetrahedral mesh element has an ID associated with it. Those IDs are constant across the tetrahedral mesh files at each time step. This allows the contribution of the adjoint photon flux from each time step to be summed in each tetrahedral mesh element.

$$\phi_{\gamma,v,h}^+ = \sum_{t_{\text{mov}}} \phi_{\gamma,v,h,t_{\text{mov}}}^+ \quad (5.1)$$

The time-integrated adjoint photon flux tetrahedral mesh is then converted back to a voxel mesh to use as input for the PyNE GT-CADIS script.

Next, the T value for each voxel, $T_{v,g,h}$, is found with Eq. 4.13. To obtain the source of photons in each photon energy group, h, single pulse irradiations are performed with ALARA. Each material in the problem is irradiated with a single energy group of neutrons, g, and allowed to decay to the time of interest. The value of $T_{v,g,h}$ is assigned to each voxel by finding the underlying material. If the voxel is composed of more than one material, the T value assigned is a volume-weighted average of the composite material.

Combining the calculated T with the time-integrated adjoint photon solution, yields the TGT-CADIS adjoint neutron source given by Eq. 4.14. The full implementation workflow is shown in Fig. 5.2.

Once the TGT-CADIS adjoint neutron source has been calculated, deterministic adjoint transport is carried out and an adjoint neutron flux Partisn file is returned. This file is then converted to a voxel mesh. This functions as an importance map for the forward neutron transport. This map will reflect the movement of geometry during the decay period and give appropriate importance to regions that contribute to the SDR at any point during geometry movement. This adjoint neutron flux mesh is used

This might need to be explained better. Maybe a picture showing showing mapping of voxel to tet mesh

should I use separate subscript for voxel?

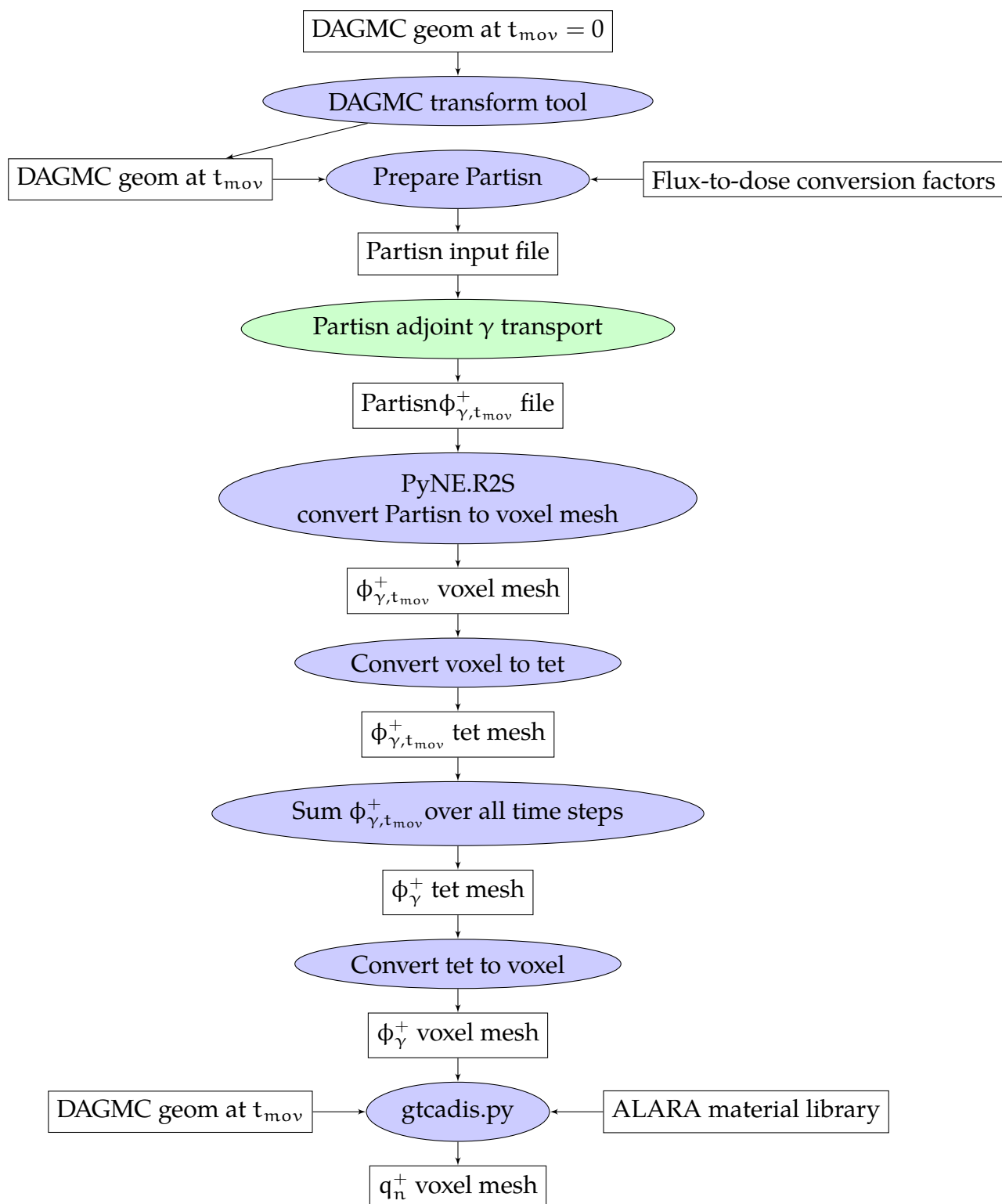


Figure 5.2: Workflow for generating the optimal adjoint neutron source via the time-integrated (T)GT-CADIS method. Scripts are shown in blue ovals, physics codes in green ovals, and files in white rectangles.

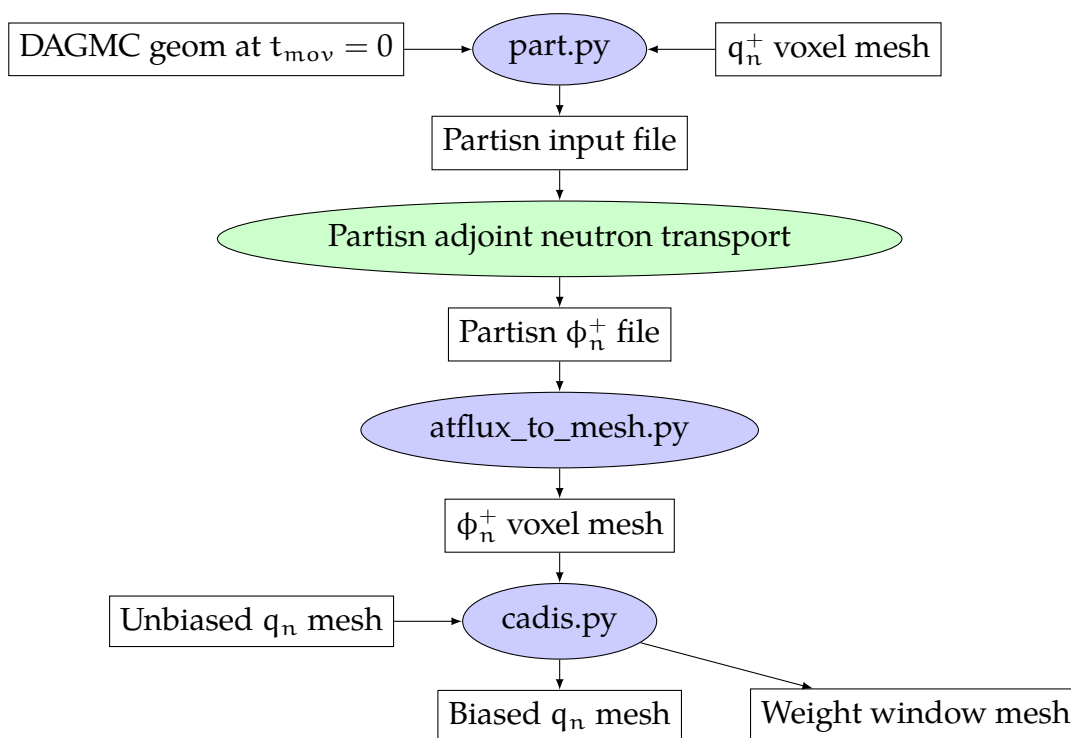


Figure 5.3: Workflow for generating a biased source and weight windows to optimize the neutron transport step. Scripts are shown in blue ovals, physics codes in green ovals, and files in white rectangles.

to generate a biased neutron source and a weight window mesh via the CADIS method.

5.2.3 Fully-optimized, Time-integrated R2S Workflow

After the biased source and weight window mesh are generated with the TGT-CADIS method, they are used to optimize the forward neutron transport step of TR2S.

The next steps of the TR2S process, from neutron transport through activation analysis are performed in the standard manner. At this point, there is a photon source tetrahedral mesh file that corresponds to the

geometry configuration at each time step of the movement.

The source mesh file in its updated position along with the previously generated adjoint photon flux mesh are used to generate a biased photon source and weight window mesh via the CADIS method. These VR parameters along with the DAGMCNP input file at each time step, t_{mov} , are all used as input for the final DAGMCNP photon transport step. This results in a SDR map for each t_{mov} .

In summary, the TGT-CADIS biased source and weight windows can be used to optimize the neutron transport and the CADIS method can be used to optimize each photon transport step. The fully optimized TR2S implementation is shown in Fig. 5.4.

5.2.4 Error Propagation

The total statistical error in the SDR arises from the MC calculations of the neutron and photon flux.

$$\sigma_{\text{SDR}}^2 = \sigma_n^2 + \sigma_\gamma^2 \quad (5.2)$$

The uncertainty in the SDR due to the uncertainty in the photon transport can be calculated during MC transport. However, the uncertainty in the SDR due to the uncertainty in the neutron MC calculation is more complicated and an area of research currently under investigation by Harb et. al [?]. This work aims to produce a methodology for propagating the error from the neutron transport to the photon source and then from the photon source to the SDR.

If a full R2S simulation is carried out, the final SDR has an error associated with the MC neutron and photon transport steps. Introducing error from the photon transport step can be avoided by not performing

Is
 $q_{\gamma, t_{\text{dec}}, t_{\text{mov}}}$
 de-
 fined
 prop-
 erly in
 text?

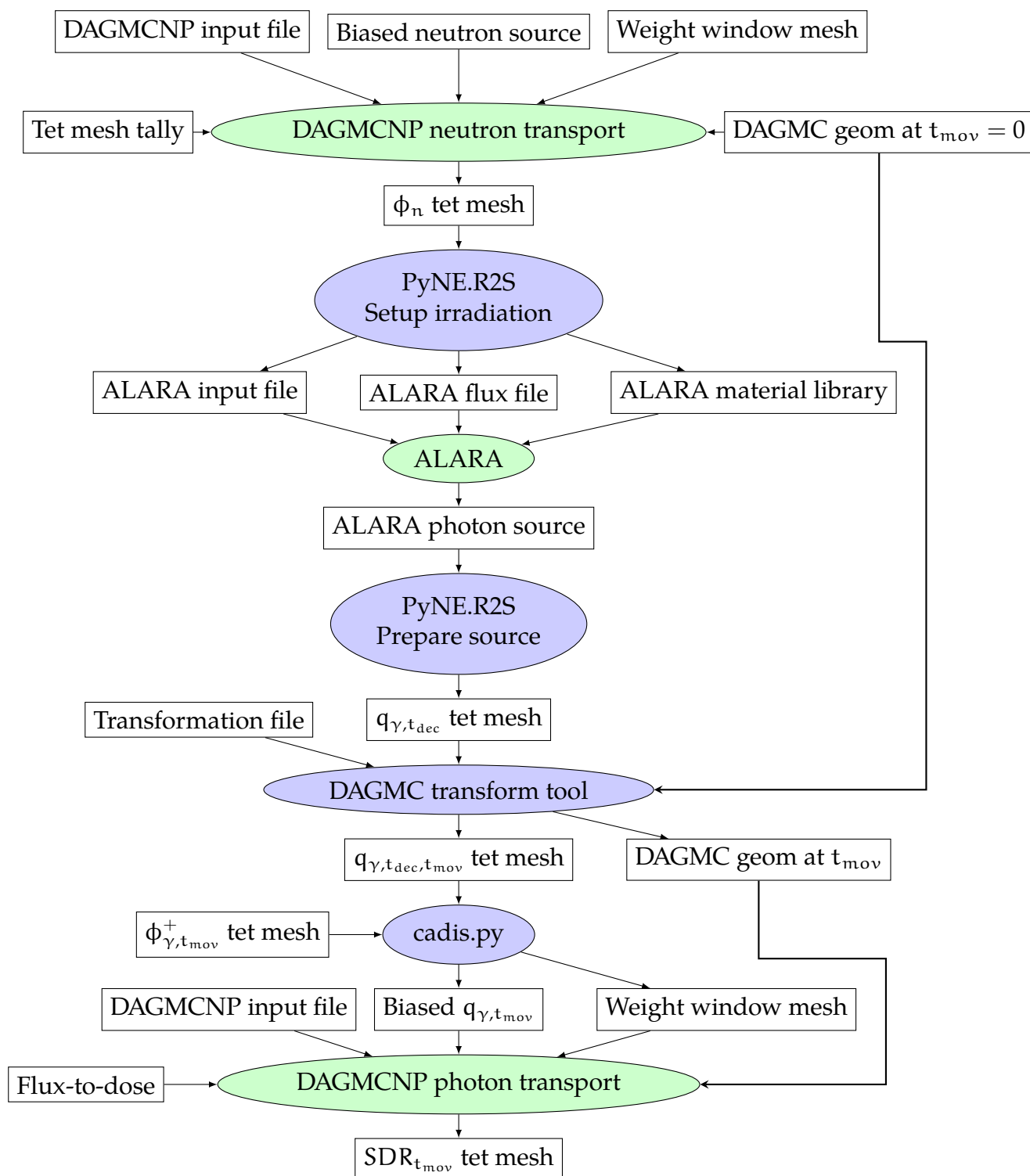


Figure 5.4: Fully optimized, time-integrated R2S workflow for calculating the SDR. This workflow uses the TGT-CADIS biased source and weight windows to optimize the neutron transport and the CADIS method to optimize the photon transport steps. Scripts are shown in blue ovals, physics codes in green ovals, and files in white rectangles.

MC photon transport and calculating the SDR using a form of Eq. 2.13

$$\text{SDR}_v = \phi_{\gamma,v}^+ q_{\gamma,v} \quad (5.3)$$

where SDR_v is the response from a discrete volume element, v . Recall that $\phi_{\gamma,v}^+$ is the result of the sum of adjoint photon flux over all time steps and required to form the TGT-CADIS adjoint neutron source and $q_{\gamma,v}$ is the photon source produced by ALARA, so both quantities are already available.

There is some relative error associated with the photon source term that originates from the MC forward neutron calculation. The relative error in the SDR, $\mathfrak{R}_{\text{SDR}}$ is then expressed as

$$\mathfrak{R}_{\text{SDR}} = \frac{1}{\text{SDR}} \sqrt{\sum_v (\text{SDR}_v \mathfrak{R}_{\text{SDR}_v})^2} \quad (5.4)$$

This error in the SDR can then be used to calculate the neutron transport FOM [?] which is important to quantifying the efficiency of TGT-CADIS.

$$\text{FOM} = \frac{\text{SDR}^2}{t_{\text{proc}} \sum_v (\text{SDR}_v \mathfrak{R}_{\text{SDR}_v})^2} \quad (5.5)$$

5.2.5 Assumptions and Practical Considerations

There are three very different time scales at play in the SDR analysis of moving systems: photon transport, geometry movement, and decay involved in the full SDR analysis of a moving system. Photon transport happens on a much faster time scale than the geometry movement, therefore it is reasonable to perform radiation transport on static step changes of the geometry configuration. It is also assumed that the time for the photon emission density to change is much longer than the period of geometry movement so the same photon source generated for a particular decay

This is shown in Elliott's prelim, but not thesis. Is this still an appropriate way to calculate the FOM?

time is used for all photon transport steps $t_{\text{mov}} = 1..N$. This assumption also allows the same T to be used at each time step of geometry movement.

In the case that the source strength is changing appreciably during geometry movement, a series of photon sources that capture these changes over time will need to be used. This will also require the calculation of different T values for each of these time steps. It is also assumed that the geometry is moving at a constant acceleration and therefore the components are located at each position for an equal amount of time. If this was not true, the sum of adjoint photon fluxes would need to be weighted by time.

The exact degree to which these assumptions about time constants hold true needs to be explored. A set of recommendations that state the criteria necessary for the TGT-CADIS method to effectively optimize the neutron transport will be established.

5.2.5.1 Data management

The fully-optimized TR2S workflow involves the generation of many large CAD geometry and volume mesh files to use for deterministic and MC transport. The decision to store or delete and regenerate all or a subset of these data files needs to be investigated.

One of the acceleration techniques employed by DAGMC is the use of Oriented Bounding Box (OBB) trees. This is a hierarchy of boxes that bound the facets of the CAD geometry. The process of building the OBB tree can be time-intensive for large geometries. Because there is a DAGMC simulation for each configuration of the geometry, a new OBB tree will be built each time. This could become rather cumbersome unless the OBB tree building is more efficient. Instead of building a new OBB tree for each geometry configuration, the OBB tree built for the original configuration could be stored and then the geometry transformation tool could be used to update the position of the boxes for each new configuration.

Figure 5.5: Geometry to be used in TGT-CADIS Demonstration.

Depending on the level of discretization in time of the motion after shut-down, there could potentially be a large number of adjoint photon transport simulations to perform. This may require the use of High Throughput Computing sources.

5.3 Demonstration

This section will outline the experiments proposed to demonstrate the utility of TGT-CADIS.

5.3.1 Toy Problem

The same geometry used in the GT-CADIS experiment shown in Chapter 3 will be used to demonstrate the efficacy of TGT-CADIS. The only difference is that a modular component of the chamber located on the far side of the detector will be moved to a location close to the detector.

First, the TR2S process without any MC VR for the neutron or photon transport steps will be applied to this problem. This will ultimately result in time-integrated SDR maps. Next, the photon transport steps will be optimized via the CADIS method. This will require deterministic adjoint photon simulations at each time step to produce VR parameters for the forward MC photon transport runs. Finally, TGT-CADIS will be applied to optimize the neutron transport step. The same adjoint photon flux solutions used in the last step can be used to calculate T which is then used to calculate the adjoint neutron source for adjoint neutron transport. The resulting adjoint neutron flux is then used to produce the VR parameters.

Missing
demo
figure

These incremental additions of optimization will be fundamental in assessing the utility of TGT-CADIS.

5.3.2 Full-scale FES Model

As the intended purpose of this work is calculating the SDR during a maintenance operation in a FES, the final challenge problem will involve the TGT-CADIS optimization of the neutron transport step of TR2S for a full-scale FES.

5.4 Summary

BIBLIOGRAPHY

- [1] A. Haghighat and J. C. Wagner, "Monte carlo variance reduction with deterministic importance functions," *Progress in Nuclear Energy*, vol. 42, no. 1, pp. 25–53, 2003.
- [2] L. Carter and E. Cashwell, *Particle-transport simulation with the Monte Carlo method*. Jan 1975.
- [3] X.-. M. C. Team, *MCNP- A General Monte Carlo N-Particle Transport Code, Version 5*. Apr 2003.
- [4] D. Valenza, H. Iida, R. Plenteda, and R. T. Santoro, "Proposal of shutdown dose estimation method by monte carlo code," *Fusion Engineering and Design*, vol. 55, no. 4, pp. 411 – 418, 2001.
- [5] R. Forrest, "Fispact-2007: User manual," *Easy Documentation Series*, vol. UKAEA FUS 534.
- [6] R. Villari and L. P. Davide Flammini, Fabio Moro, "Development of the advanced d1s for shutdown dose rate calculations in fusion reactors," *Transactions of the American Nuclear Society*, vol. 116, pp. 255–258, 2017.
- [7] Y. Chen and U. Fischer, "Rigorous mcnp based shutdown dose rate calculations: computational scheme, verification calculations and application to iter," *Fusion Engineering and Design*, vol. 63, pp. 107 – 114, 2002.
- [8] A. Davis and R. Pampin, "Benchmarking the mcr2s system for high-resolution activation dose analysis in iter," *Fusion Engineering and Design*, vol. 85, no. 1, pp. 87 – 92, 2010.
- [9] E. D. Biondo, A. Davis, and P. P. Wilson, "Shutdown dose rate analysis with cad geometry, cartesian/tetrahedral mesh, and advanced

- variance reduction," *Fusion Engineering and Design*, vol. 106, no. Supplement C, pp. 77 – 84, 2016.
- [10] J. C. Wagner, D. E. Peplow, and S. W. Mosher, "Fw-cadis method for global and regional variance reduction of monte carlo radiation transport calculations," *Nuclear Science and Engineering*, vol. 176, no. 1, pp. 37–57, 2014.
 - [11] A. M. Ibrahim, D. E. Peplow, R. E. Grove, J. L. Peterson, and S. R. Johnson, "The multi-step cadis method for shutdown dose rate calculations and uncertainty propagation," *Nuclear Technology*, vol. 192, pp. 286 – 298, 2015.
 - [12] J. W. Durkee, R. C. Johns, and L. S. Waters, "Mcnp6 moving objects part i: Theory," *Progress in Nuclear Energy*, vol. 87, no. Supplement C, pp. 104 – 121, 2016.
 - [13] J. W. Durkee, R. C. Johns, and L. S. Waters, "Mcnp6 moving objects. part ii: Simulations," *Progress in Nuclear Energy*, vol. 87, no. Supplement C, pp. 122 – 143, 2016.
 - [14] E. D. Biondo and P. P. H. Wilson, "Transmutation approximations for the application of hybrid monte carlo/deterministic neutron transport to shutdown dose rate analysis," *Nuclear Science and Engineering*, vol. 187, no. 1, pp. 27–48, 2017.
 - [15] E. Lewis and W. Miller, *Computational Methods of Neutron Transport*. American Nuclear Society, Inc., 1993.
 - [16] T. Eade, S. Lilley, Z. Ghani, and E. Delmas, "Movement of active components in the shutdown dose rate analysis of the iter neutral beam injectors," *Fusion Engineering and Design*, vol. 98-99, no. Supplement C, pp. 2130 – 2133, 2015. Proceedings of the 28th Symposium On Fusion Technology (SOFT-28).

- [17] R. ALCOUFFE, R. BAKER, J. DAHL, S. TURNER, and R. WARD, "Partisn: A time-dependent, parallel neutral particle transport code system," may 2005.
- [18] T. Tautges, P. Wilson, J. Kraftcheck, B. F Smith, and D. Henderson, "Acceleration techniques for direct use of cad-based geometries in monte carlo radiation transport," may 2009.
- [19] R. Morris and C. McBride, "Trelis 16.4 user documentation," *csimsoft*, 2013-2017.
- [20] P. Wilson, H. Tsige-Tamirat, H. Khater, and D. Henderson, "Validation of the alara activation code," vol. 34, p. 784, 01 1998.
- [21] ICRP, "Conversion coefficients for use in radiological protection against external radiation," *ICRP Publication 74. Ann. ICRP*, vol. 26, pp. 3-4.
- [22] E. Sartori and G. Panini, "Zz groupstructures, vitamin-j, xmas, ecco-33, ecco2000 standard group structures," vol. Tech. Rep. 40-03, 1991.
- [23] C. Bates, E. Biondo, and K. Huff, "Pyne progress report," 11 2014.
- [24] A. Pashchenko and H. Wienke, "The processed fendl-2 neutron activation cross-section data files summary documentation," *www-nds.iaea.org*, 1997.